A comparison of the Dielectric Function for p-point Water Models

Noah Shevy,[1] Prapti Kakkar,[1] and Alex Travesset[2]
[1)]*Ames National Laboratory, and Department of Chemical and Biological Engineering, Iowa State University, Ames, Iowa 50011*
[2)]*Department of Physics and Astronomy, Iowa State University and Ames National Laboratory, Ames, IA, 50011*

(*Corresponding author: trvsst@ameslab.gov)

(*Electronic mail: prapti@iastate.edu.)

(*Electronic mail: noahshevy@gmail.com)

(Dated: August 4, 2026)

We compute the longitudinal dielectric function $\varepsilon_l(k)$ for p-point water models, p=3 (SPC/E, TIP3P), p=4 (TIP4P-EW, OPC) and p=5 (TIP5P-E) from the charge-charge fluctuation function $S_{ZZ}(k)$, obtained from two methods: average of the charge in k-space (method:sum) and from the pair distribution function in Fourier space (method:integral). The latter requires a continuation to small k-values, which we thoroughly discuss. We conclude with a detailed comparison of the longitudinal dielectric function for the different p-point models and its main characteristics: small k and large k limits, position of the poles and its (complex) zeros.

I. INTRODUCTION

The static dielectric constant ε_w is just the long-wavelength limit of the (longitudinal) dielectric function $\varepsilon_l(k)$. For water, $\varepsilon_l(k)$ was first calculated in Ref.[1] by a combination of simulations using the Bopp-Jancsó-Heinzinger model and neutron scattering experiments. Other determinations include the TIP4P model[2] and other organic solvents[3]. More recently, two of us in this paper have calculated it[4] for the SPC/E model[5].

The dielectric function $\varepsilon_l(k)$ is extremely important as it determines the electrostatic interaction of any number of charges in a medium. Ref.[4], has shown that the Coulomb potential created by a point charge of valence (or charge number) Q takes the form (we denote the unit of charge as e_L)

$$\phi(r)=\frac{e_L Q}{4\pi\varepsilon_0 r}\left(\frac{1}{\varepsilon_w}+\sum_{l=1}\zeta_l e^{-k_{I,l}r}\cos(k_{R,l}r+\alpha_l)\right), \quad (1)$$

where l runs over all zeros of the dielectric function, i.e $\varepsilon_l(k_l)=0$, where $k_l=k_{R,l}+ik_{I,l}$ and ζ_l,α_l are real numbers, defined as the modulus and phase of the complex number

$$\zeta_l e^{i\alpha_l}=4\mathrm{Res}\left(\frac{1}{\varepsilon_l(k_l)}\right), \quad (2)$$

where Res stands for the residue in the complex plane. Therefore, the dielectric function modifies the Coulomb law by adding a damped oscillatory component. Only if there are no zeros of $\varepsilon_l(k)$, or for sufficiently long distances, $r>>\frac{1}{k_{I,l}}$ we recover the usual Coulomb law in a medium with dielectric constant ε_w, namely

$$\phi(r)=\frac{e_L Q}{4\pi\varepsilon_0\varepsilon_w r}. \quad (3)$$

The additional contribution in Eq. 1 reflects the role played by discrete water molecules, so we expect, on physical grounds, that $|k_l|\sim\frac{\pi}{D_w}$, where D_w is the diameter of a water molecule.

The purpose of this paper is to obtain, compare and discuss $\varepsilon_l(k)$ for p-point models, see Fig. 1. More concretely, we investigate the SPC/E[5] and TIP3P[6] (p=3), TIP4P-Ew[7], OPC[8](p=4) and TIP5P-E[9] (p=5).

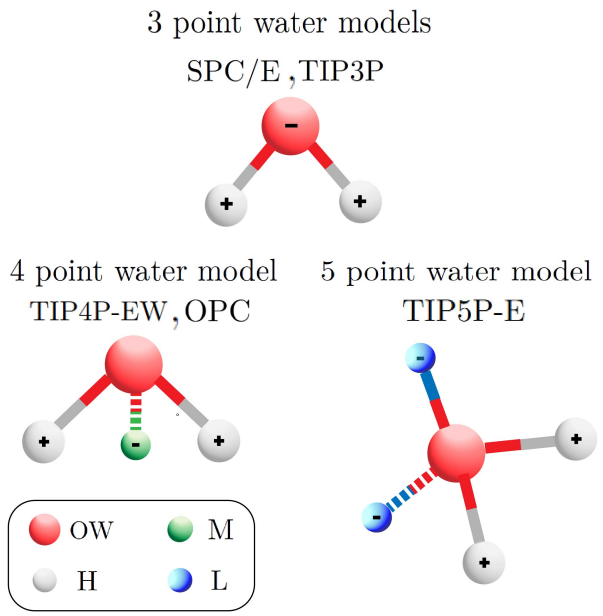

Figure 1: Representation of the p-point models studied in this paper with the conventional names given to the different p-points.

II. METHODS

The dipole moment for a p-point water model is given as

$$\mu_w=\begin{cases}2e_L q_H d_{O-H}\cos(\theta/2) & 3\\ 2e_L q_H(d_{O-H}\cos(\theta/2)-d_{O-M}) & 4\\ 2e_L\left(q_H d_{O-H}\cos(\theta_H/2)+q_L d_{O-L}\cos(\theta_L/2)\right) & 5\end{cases} \quad (4)$$

which is derived from Fig. 1.

The dielectric function is computed from the fluctuation formula assuming tin-foil boundary conditions, see Ref.[4,10]

$$\varepsilon_l(k) = \left(1 - 9py\frac{S_{ZZ}(k)}{k^2\mu_w^2}\right)^{-1} \tag{5}$$

$y = \frac{n_w\mu_w^2}{9k_BT\varepsilon_0}$ and n_w is the water number density. The function $S_{ZZ}(k)$, the charge-charge correlation function, can be computed in two different ways:

$$S_{ZZ}(k) = \begin{cases} \frac{1}{pN_w}\langle\hat{\rho}_Z(\boldsymbol{k})\hat{\rho}_Z(-\boldsymbol{k})\rangle & \text{method:sum} \\ e_L^2\sum_\mu\sum_\nu q_\mu q_\nu S_{\nu\mu}(\boldsymbol{k}) & \text{method:integral} \end{cases} . \tag{6}$$

The first method is dubbed :sum as it involves the sum over all charge positions, see Eq. 8, while the second :integral as it involves the Fourier Transform Eq. 10.

Here, we consider water as composed of S species, i.e. O, H, L, etc.., see Fig. 1. The first (method:sum) requires averaging

$$\hat{\rho}_Z(\boldsymbol{k}) = \sum_{\nu=1}^{S} q_\nu\hat{\rho}_\nu(\boldsymbol{k}) \tag{7}$$

where

$$\hat{\rho}_\nu(\boldsymbol{k}) = \sum_{j=1}^{N_\nu} e^{-i\boldsymbol{k}\cdot\boldsymbol{r}_j} . \tag{8}$$

This is the method used in Ref.[4],and our implementation here follows the same procedure, so we refer there for details.

The second way (method:integral), was briefly mentioned in Ref.[4],but never applied to obtain the dielectric function, so we discuss it here in detail. It can be formulated as

$$e_L^2\sum_\mu\sum_\nu q_\mu q_\nu S_{\nu\mu}(\boldsymbol{k}) = \begin{cases} \frac{4}{3}q_H^2e_L^2\left(\frac{3}{2} + \hat{h}_{OO}(k) - 2\hat{h}_{OH}(k) + \hat{h}_{HH}(k)\right) & \text{3 point} \\ q_H^2e_L^2\left(\frac{3}{2} + \hat{h}_{MM}(k) - 2\hat{h}_{MH}(k) + \hat{h}_{HH}(k)\right) & \text{4 point} \\ \frac{4}{5}q_H^2e_L^2\left(1 + \hat{h}_{LL}(k) - 2\hat{h}_{LH}(k) + \hat{h}_{LL}(k)\right) & \text{5 point} \end{cases} , \tag{9}$$

which requires the pair distribution function $h_{IJ}(r) = g_{IJ}(r) - 1$ in k-space, defined through the dimensionless Fourier transform $\hat{f}$, i.e the radial Fourier transform, given as

$$\hat{f}(k) = n_w\int_0^\infty drr^2 4\pi f(r)\frac{\sin(kr)}{kr} . \tag{10}$$

Note that with this definition of the radial Fourier transform, it is,within the NVT ensemble, $\hat{h}_{OO}(0) = -1$, $\hat{h}_{HH}(0) = -\frac{1}{2}$ and $\hat{h}_{MM}(0) = -1$, $\hat{h}_{LL}(0) = -\frac{1}{2}$ with $\hat{h}_{IJ}(0) = 0$ if $I \neq J$.Within the grand canonical ensemble, these limits are defined in terms of the thermodynamic compressibility and others, which are computed through the Kirkwood-Buff method[11–13].

It is convenient to introduce intramolecular(m) and intermolecular(d) contributions[1], which we will denote with the *md* notation, and write

$$S_{ZZ}(\boldsymbol{k}) = S_{ZZ}^{(m)}(\boldsymbol{k}) + S_{ZZ}^{(d)}(\boldsymbol{k}) . \tag{11}$$

The intramolecular contribution can be computed analytically as

$$S_{ZZ}^{(m)}(k) = \begin{cases} \frac{2}{3}q_H^2e_L^2\left(3 + \frac{\sin(kd_{HH})}{kd_{HH}} - 4\frac{\sin(kd_{OH})}{kd_{OH}}\right) & \text{3 point} \\ \frac{1}{2}q_H^2e_L^2\left(3 + \frac{\sin(kd_{HH})}{kd_{HH}} - 4\frac{\sin(kd_{MH})}{kd_{MH}}\right) & \text{4 point} \\ \frac{2}{5}q_H^2e_L^2\left(2 + \frac{\sin(kd_{HH})}{kd_{HH}} - 4\frac{\sin(kd_{LH})}{kd_{LH}} + \frac{\sin(kd_{LL})}{kd_{LL}}\right) & \text{5 point} \end{cases} \tag{12}$$

The charge fluctuation $S_{ZZ}(k)$ has exact forms in both long and small wavelength limits[4].

$$S_{ZZ}(k) \approx S_{ZZ}^{(m)}(k), \quad k >> k_c \tag{13}$$

$$S_{ZZ}(k) \approx \frac{\mu_w^2}{9py}\left(\frac{\varepsilon_w - 1}{\varepsilon_w}\right)k^2 + b_4k^4 + \cdots, \quad k \to 0 \tag{14}$$

The long wavelength limit is defined from $k_c = \frac{2\pi}{d_{HH}}$ with d_{HH} the distance between the two hydrogens. The small wavelength limit is constrained by Stillinger-Lovett (SL) sum rules, where $\varepsilon_w = \varepsilon_l(k=0)$ is the static dielectric constant and b_4 a coefficient. The SL limit implies for $p = 3$ the sum rules

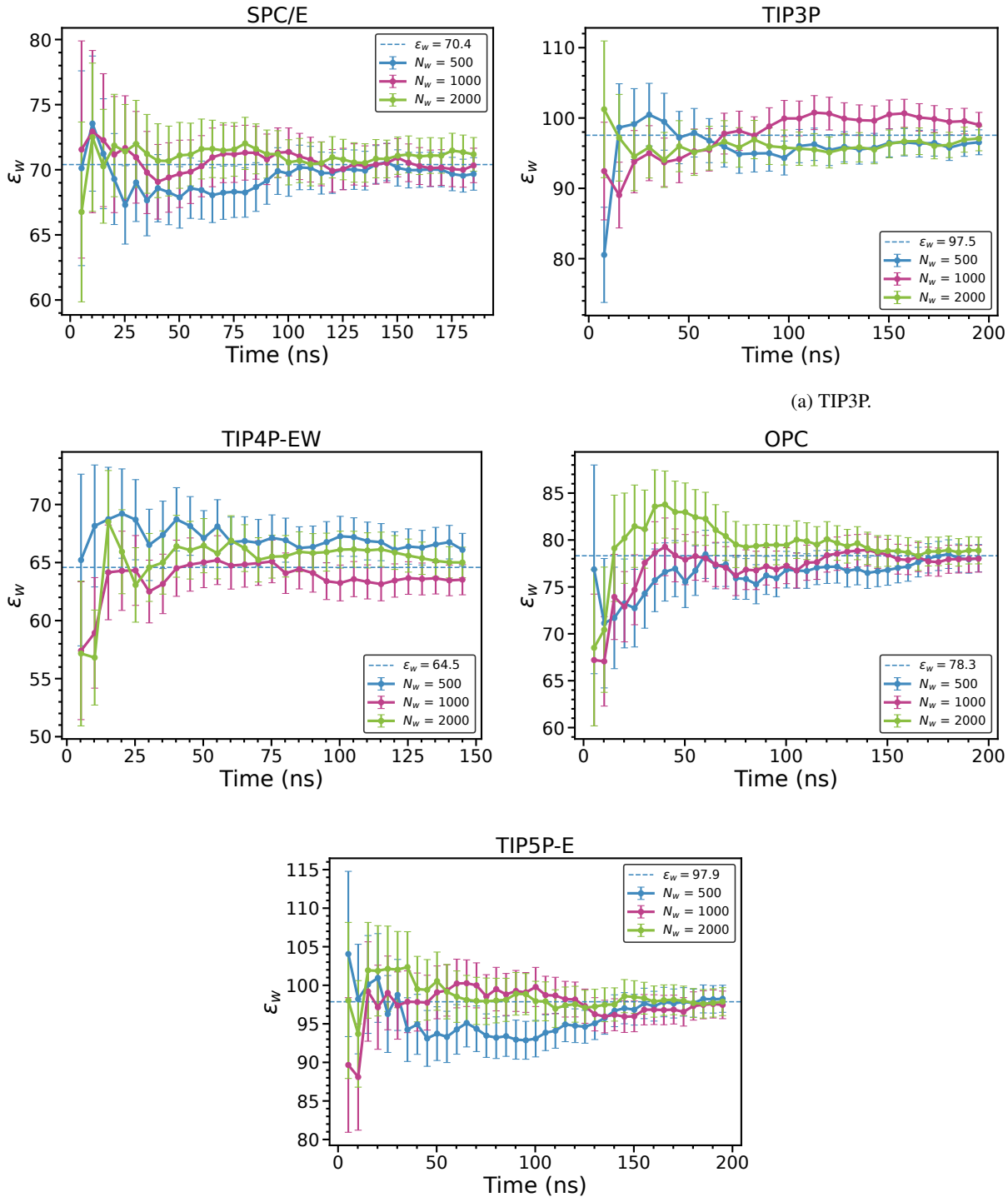

(a) TIP3P.

Figure 2: Summary of calculations for the static dielectric constant ε_w in NPT. Cumulative average value and error is also shown.

$$-\frac{3}{2} = 4\pi n_w \int_0^\infty dr r^2 \left(h_{OO}(r) - 2h_{OH}(r) + h_{HH}(r)\right) \quad (15)$$

$$\frac{-1}{6y}\left(\frac{\varepsilon_w - 1}{\varepsilon_w}\right)\frac{\mu_w^2}{q_H^2 e_L^2} = 4\pi n_w \int_0^\infty dr r^4 \left(h_{OO}(r) - 2h_{OH}(r) + h_{HH}(r)\right)$$

$$90\frac{b_4}{q_H^2} = 4\pi n_w \int_0^\infty dr r^6 \left(h_{OO}(r) - 2h_{OH}(r) + h_{HH}(r)\right)$$

These sum rules are used in method:integral to constrain the long distance limit for $h_{IJ}(r)$. SI provides a more explicit derivation.

The static dielectric constant, which is needed for Eq. 14 is calculated from the flucutation formula[14]

$$\varepsilon_w - 1 = \frac{\langle \vec{M}^2 \rangle}{3\varepsilon_0 k_B T V} = \frac{n_w}{3\varepsilon_0 k_B T}\mu_w^2 g = 3y\frac{\langle \vec{M}^2 \rangle}{N\mu_w^2}\,, \quad (16)$$

see Ref.[4] for a discussion.

III. SIMULATION DETAILS

The quantity y, defined in Eq. 5 has the value

$$y = y(298.15, r)\frac{\rho_w(T,P)}{10^3}\frac{298.15}{T} \quad (17)$$

where $y(298.15, r)$ is computed at a reference value of $T = 298.15$K and $\rho_{w,r} = 10^3$ kg/m^3. Here, $\rho_w(T,P)$ is the density of water (in kg/m^3) at the corresponding temperature and pressure. The error of $y(298.15, r)$ is on the last digit, which comes from the last digit of the water molecular weight ($M_w = 18.01528$ g/mol) uncertainty. Table I provides actual numerical values.

Model	p	μ_B (e_L·Å)	$y(298.15, r)$	ρ_w (kg/m^3)	y
SPC/E	3	0.48937	6.177675	0.985(8)	6.196208
TIP3P	3	0.48863	6.166262	0.986(9)	6.079934
TIP4P-EW	4	0.48321	6.070332	0.995(6)	6.046050
OPC	4	0.51625	6.912483	0.997(8)	6.891746
TIP5P-E	5	0.47720	5.973980	1.003(9)	5.991902

Table I: Actual values for Eq. 17 for all water models analyzed.

The standard deviation s_D and error s_E for a quantity A in a simulation run for a time T_s and including N_T configurations is given as

$$s_D(A) = \frac{1}{N_T - 1}\sum_{l=1}^{N_T}(A_l - \overline{A})^2 \quad , \quad \overline{A} = \frac{1}{N_T}\sum_{l=1}^{N_T} A_l$$

$$s_E(A) = s_D(A)\left(\frac{2\tau_A}{T_s}\right)^{1/2}\,, \quad (18)$$

here τ_A is the autocorrelation time for the observable

$$C_{AA}(t) = \frac{\langle A(t)A(0)\rangle - \langle A(0)\rangle^2}{\langle A(0)^2\rangle - \langle A(0)\rangle^2}\,. \quad (19)$$

In practice, that data was collected so that for successive intervals it was found that $s_E(A) = s_D(A)$.

Simulations used HOOMD-blue[15,16] using v4.7 implemented through HOODLT[17,18]. HOODLT was used to generate the initial configurations, implement the force field and analyze the results. Water was modeled with the different models using rigid body dynamics, as implemented in HOOMD-blue[19,20].

NPT simulations used the MTTK thermostat and barostat with thermostat and barostat coupling times $\tau_T = 0.01$ ps and $\tau_P = 0.1$ ps, and a time step $\Delta t = 1$ fs. We verified that the instantaneous kinetic temperature remains stable about the target value with no drift throughout the production runs under this MTTK coupling as shown in Fig. **??**. Electrostatic interactions were included by the PPPM method with order of 4 and grid dimensions of $128 \times 128 \times 128$. The cut-off for the Lennard Jones particles was set to 2.8σ and electrostatic cut-off (R_{max}) for different systems is provided in Table II.

IV. RESULTS AND DISCUSSION

A. Static Dielectric Constant

Fig. 2 shows the convergence of the static dielectric constant, computed from Eq. 16, as a function of simulation time (in ns). It follows the same trends discussed in the literature, as discussed in Ref.[4]. The results are summarized in Table II. These values will be used to obtain the low k limit for both $S_{ZZ}(k), \varepsilon_l(k)$, as discussed below.

The values calculated from our simulations are consistent with the ones reported in the literature. For SPC/E, Ref.[4] has calculated $\varepsilon_w = 70.0(4)$ at $T = 300$ K. For the other water models, Ref.[21] quotes the following values at $T = 298$: $\varepsilon_w = 95$ (TIP3P), $\varepsilon_w = 63$ (TIP4P-EW) and $\varepsilon_w = 92$ (TIP5P-E). These values are slightly lower, albeit consistent, with our quoted results. Ref.[22] provide some additional discussion for these effects. Ref.[8] quotes $\varepsilon_w = 78.4(6)$ for OPC, consistent with our estimates.

B. Dielectric Function

1. *Calculation of* $\varepsilon_l(k)$

We have described two methods, see Eq. 6. Method:sum has been extensively discussed in Ref.[4], so here we describe method:integral. Concentrating on TIP3P (see other cases in

Model	N_w	t(ns)	R_{max} (nm)	α (nm^{-1})	P (bar)	s_D	s_E	T	ε_w
SPC/E	500	200	1	3.77	11.1 (14.1)	53.77	1.22	298	69.7
	1000	200	1.2	3.12	-3.1 (9.7)	56.79	1.29	298	70.3
	2000	190	1.4	3.03	2.3 (6.9)	55.58	1.29	298	71.2
TIP3P	500	250	1	4.30	10.6 (11.0)	79.07	1.61	298	96.5
	1000	230	1.2	3.12	-2.4 (8.4)	79.42	1.68	298	99.0
	2000	191	1.2	3.03	1.8 (6.4)	77.54	1.81	298	97.1
TIP4P-EW	500	150	1	4.30	19.4 (15.7)	52.78	1.39	298	64.9
	1000	210	1.2	3.12	1.1 (9.4)	50.59	1.12	298	64.3
	2000	163	1.2	3.03	-2.1 (7.6)	49.54	1.25	298	64.6
OPC	500	200	1	3.77	-6.9 (14.3)	64.26	1.46	298	78.1
	1000	200	1	3.66	5.3 (10.2)	63.50	1.11	298	78.7
	2000	200	1	3.55	9.2 (7.2)	63.26	1.43	298	78.9
TIP5P-E	500	200	1	3.77	-8.6 (12.6)	77.53	1.76	298	98.2
	1000	200	1.2	3.12	24.4 (9.4)	79.05	1.79	298	97.5
	2000	200	1.2	3.03	17.1 (6.4)	80.07	1.81	298	97.9

Table II: Static dielectric constant at 1 bar. R_{max} is the cut-off in the local electrostatic contribution and α the split parameter between real and k-space. P is the final pressure. s_D is the standard deviation and s_E the standard error.

SI from Fig.**??**-**??**) we derived, see discussion after Eq. 10: $\hat{h}_{HH}(k=0) = -\frac{1}{2}, \hat{h}_{OO}(k=0) = -1, \hat{h}_{OH}(k=0) = 0$. The results obtained from the simulation are shown in Fig. 3(solid lines) and deviate from the expected exact result.

These deviations are expected, because in a simulation, the smallest non-zero value that can be attained is $k \approx \frac{\pi}{L}$, where $V = L^3$ is the volume of the simulation box, and therefore the integral over large distances in Eq. 10 is not possible to calculate as it involves values of k that cannot be simulated.

The SL sum rules Eq. 15 provide a way around to the above limitation. We expand of $\hat{h}_{IJ}(k)$ for small k according to

$$\hat{h}_{IJ}(k) = f^{(0)} + f_{IJ}^{(2)} k^2 + f_{IJ}^{(4)} k^4 + \cdots .. \tag{20}$$

where $f^{(0)}$ is known from the normalization condition. We then establish an interval $[k_{min}, k_{max}]$ where Eq. 20 is satisfied, and use to fit the coefficients with the additional constraint that the SL Eq. 14 is satisfied. Further details on how this is done are provided in the SI. Fig. 3 shows the corrected values for $\hat{h}_{IJ}(k)$. This is how the small k limit for $\hat{h}_{IJ}(k)$ is fixed.

The resulting charge-charge fluctuation function $S_{ZZ}(k)$ is shown in Fig. 4. Both method:integral and method:sum give the same results, see Fig. 4a; Method:integral gives smoother results, yet the low k limit requires a more sophisticated, as described above, correction.

The coefficient b_4 in SL Eq. 14 is obtained by three different methods: The fit to method:sum as in our previous publication[4], the determination from $f_{IJ}^{(4)}$ coefficients, see Eq. 20, according to

$$b_4 = \frac{4q_H^2}{3}\left(f_{OO}^{(4)} - 2f_{OH}^{(4)} + f_{HH}^{(4)}\right) \tag{21}$$

see derivation in SI, and finally a straight fit to the uncorrected low k-dependence from method integral. The actual results

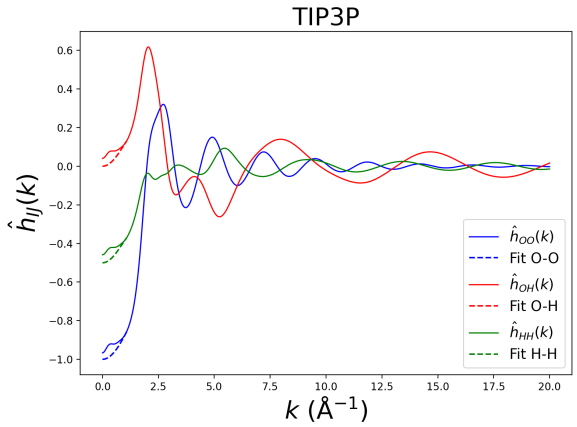

Figure 3: Calculation of $\hat{h}_{IJ}(k)$ for the TIP3P model. The dashed line is the corrected low k dependence obtained from a fit to Eq. 20 as described in the text. Further considerations and details of the derivation are provided in SI.

are consistent with values

$$b_4 = \begin{cases} 5.1 \cdot 10^{-4} \text{Å}^4 e^2 & \text{method:sum} \\ 6.4 \cdot 10^{-4} \text{Å}^4 e^2 & \text{method:Integral Eq. 21} \\ 5.8 \cdot 10^{-4} \text{Å}^4 e^2 & \text{method:Integral, fit to bare} S_{ZZ}(k) \end{cases} \tag{22}$$

Here, $b_4 = 5.1 \cdot 10^{-4}$ is the more reliable number as method sum gives more consistent results. Table III provides a summary of the b_4 coefficients for the different models.

2. $\varepsilon_l(k)$ for p-point models

Fig. 5a shows $S_{ZZ}(k)$ for all five water models considered in this study. Plots for each individual model are provided in

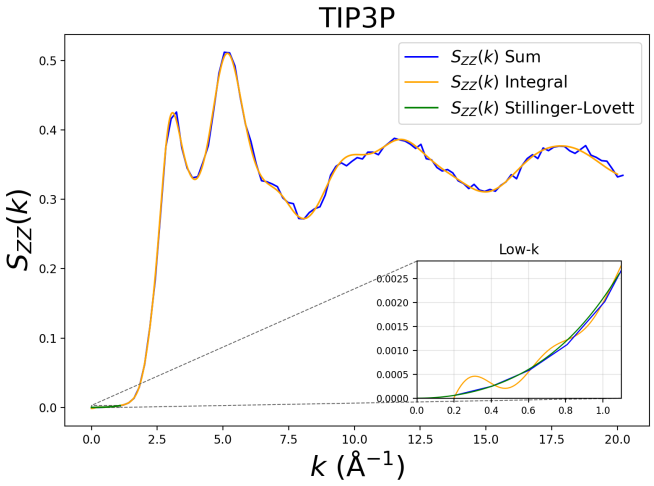

(a) $S_{ZZ}(k)$ computed with method:sum and method:integral.

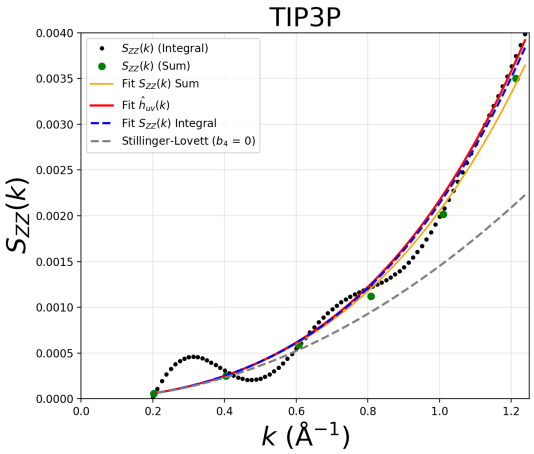

(b) Analysis of the low k dependence of $S_{ZZ}(k)$ and the determination of the b_4-coefficient, defined in Eq. 14.

Figure 4: Calculation of the charge-charge fluctuation $S_{ZZ}(k)$.

Units	b_4 Å$^4 e_L^2$	pole 1 Å^{-1}	pole 2 Å^{-1}	k_s Å^{-1}	ζ	α rad
SPC/E	$3.8\cdot10^{-4}$	0.233	16.21	$3.12+0.58i$	14.23	0.98
TIP3P	$6.0\cdot10^{-4}$	0.155	14.7	$2.87+0.73i$	17.70	1.26
TIP4P-EW	$3.1\cdot10^{-4}$	0.126	20.1	$3.15+0.58i$	17.40	0.89
OPC	$4.8\cdot10^{-4}$	0.159	24.9	$3.13+0.56i$	21.19	0.79
TIP5P-E	$1.1\cdot10^{-4}$	0.275	8.18	$2.70+0.64i$	5.74	1.63

Table III: Summary of b_4 coefficients, poles, complex zeros $k_s = k_R + ik_I$, and residue parameters ζ and α for $\varepsilon_l(k)$ for all water models.

SI. From Eq. 12, for large values of k it is

$$S_{ZZ}(k) = \begin{cases} 2q_H^2 e_L^2 & \approx 0.359 e_L^2 \quad \text{SPC/E} \\ 2q_H^2 e_L^2 & \approx 0.348 e_L^2 \quad \text{TIP3P} \\ \frac{3}{2} q_H^2 e_L^2 & \approx 0.412 e_L^2 \quad \text{TIP4P-EW} \\ \frac{3}{2} q_H^2 e_L^2 & \approx 0.692 e_L^2 \quad \text{OPC} \\ \frac{4}{5} q_H^2 e_L^2 & \approx 0.046 e_L^2 \quad \text{TIP5P-E} \end{cases} \tag{23}$$

It is noteworthy that the value for TIP5P is an order of magnitude smaller than the other cases, which explains the overall smaller $S_{ZZ}(k)$ for TIP5P-E in Fig. 5a.

In order to avoid the distorting effect of the poles when presenting $\varepsilon_l(k)$, we show the results in terms of

$$\chi(k) = 1 - \frac{1}{\varepsilon_l(k)} \ , \tag{24}$$

which satisfies $\chi(0) = \frac{\varepsilon_w - 1}{\varepsilon_w}$ and $\chi(\infty) = 0$. There are consistent peaks at $k \approx \frac{2\pi}{d_c} \approx 3$, which reflect the size of the water molecule and of its dipole moment. Here again, the case of TIP5P-E is special with a function χ which is much smaller than the other cases.

Table III summarizes relevant parameters characterizing $\varepsilon_l(k)$. The coefficient b_4, which characterizes the low$-k$ limit for $\varepsilon_l(k)$, see Eq 13 is consistently smaller as p increases. The poles of $\varepsilon_l(k)$ are at around $k \sim 0.1-0.3$ Å^{-1} for the first and $k \sim 10-20$ Å^{-1} for the second for all p-models.

The zeros of $\varepsilon_l(k)$, i.e.

$$\varepsilon_l(k_s) = 0 \quad \text{with } k_s = k_R + k_I i \tag{25}$$

determine the short-distance form of the Coulomb law, see Eq. 1, see also Eq 2. As shown in Ref.[4], if k_s is a zero, inversion symmetry and the fact that $\varepsilon_l(k)$ is real for k real implies that each zero has multiplicity of four; if k_s is a zero, then $-k_s$, k_s^*,$-k_s^*$, where a^* is the complex conjugate of a, are also zeros.

The zeros were computed in two different ways. In the first, we computed the integral in Eq. 1 numerically, and fitted to the expected form (the rhs). In the second we parameterized the dielectric function as described in Ref.[4] and computed the poles and residues by analytical continuation. Both methods gave very similar results for k_s, but some small discrepancies were found for the residue coefficients (Eq. 2). Table III summarizes the results obtained with the first method. With small variations, the zeros k_s are such that $k_{s,R} \approx 3$ and $k_{s,I} \approx 0.6$ in Å^{-1} for all models, also in agreement with Ref.[4]. The results for the residue coefficient show much larger variability.

V. CONCLUSIONS

The longitudinal dielectric function $\varepsilon_l(k)$ describes the role of the water molecule finite size, thus determining the short-range electrostatic force among charges, see Eq. 2. It is directly measurable from neutron experiments and indirectly,

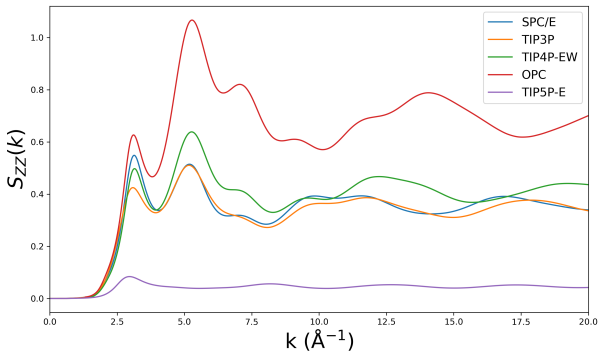

(a) $S_{ZZ}(k)$ for all models

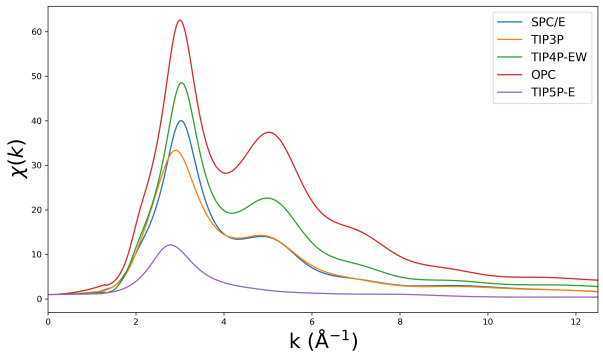

(b) $\chi(k)$ for all models

Figure 5: Comparison between $S_{ZZ}(k)$ and $\chi(k)$ for all water models considered in this study.

from other techniques, such as the surface force apparatus, which can measure forces directly.

In this paper, we have provided a detailed calculation of the longitudinal dielectric function $\varepsilon_l(k)$ for water with five different p-point models: SPC/E, TIP3P, TIP4P-EW, TIP5P-E and OPC, using two different methods, method:sum and method:integral combined with the small-k limit, see Eq. 13. Both methods give entirely consistent results and satisfy the large k limit described by Eq. 12. Application of both methods enables to estimate the errors. The most relevant parameters characterizing $\varepsilon_l(k)$ are provided in Table III.

We have provided an accurate determination of the dielectric constant ε_w for the different p-models. This is necessary for obtaining the correct limit for $\varepsilon_l(k)$ at low k-values. It is relevant to state that besides OPC, which was determined to reproduce electrostatic properties accurately, only the SPC/E has a dielectric constant consistent with real water. There are large variations of dielectric constant among models, and not surprisingly, the different $\varepsilon_l(k)$ functions show large variations as well.

The next step is to compare Eq. 1, see also Eq. 2, with the potential of mean force in real simulations, see for example Ref.[23,24], where charges have a finite diameter. We can anticipate that while the values of k_s quoted in Table III reproduce well the simulations, the residue coefficients ζ, α are not entirely consistent. It is beyond the scope of this paper to analyze this situation, but it will be discussed elsewhere.

At this point, it would be of great interest to revisit the determination of the low-k limit in $\varepsilon_l(k)$ Ref.[1] by Bopp et al. and improve its accuracy, as the results seem to imply that $\varepsilon_l(k)$ has a minimum for small k, between the $k = 0$ limit and the first pole. This is different from the rigid p-point models considered in this paper, where $\varepsilon_l(k)$ is monotonically increasing towards the first pole, similarly as in other simpler models, such as a LJ with point dipoles (Stockmayer model)[25]. Of course, it would also be of great interest to determine the longitudinal dielectric function with polarizable water models.

ACKNOWLEDGMENTS

NS acknowledges a DOE SULI internship over fall 2025. Research supported by the U.S. Department of Energy (U.S. DOE), Office of Basic Energy Sciences, Division of Materials Sciences and Engineering. Ames National Laboratory is operated for the U.S. DOE by Iowa State University under Contract DE-AC02-07CH11358. This work used EXPANSE and BRIDGES2 through allocation MCB140071 from the Advanced Cyberinfrastructure Coordination Ecosystem: Services Support (ACCESS) program[26], which is supported by National Science Foundation grants 2138259, 2138286, 2138307, 2137603, and 2138296.

DATA AVAILABILITY STATEMENT

The data that support the findings of this study are available from the corresponding author upon reasonable request.

SUPPLEMENTARY MATERIAL

The supplementary material contains one supporting information file. Included is discussion of the low k limit of $S_{ZZ}(k)$ using Stillinger-Lovett relations by explaining the Fourier transform used to calculate $\hat{h}(k)$. We also present a table of $f_{XY}^{(i)}$ for all models which highlights the specific values we obtained through our simulations. Lastly, additional results illustrating differences between SPC/E, TIP3P, TIP4P-EW, OPC, and TIP5P via plots of $g_{OO}(r)$, $\chi(k)$, and $\varepsilon_l(k)$ are shown.

REFERENCES

[1] P. A. Bopp, A. A. Kornyshev, and G. Sutmann, "Static Nonlocal Dielectric Function of Liquid Water," Physical Review Letters **76**, 1280–1283 (1996).
[2] I. P. Omelyan, "Longitudinal wavevector- and frequency-dependent dielectric constant of the TIP4P water model," Molecular Physics **93**, 123–136 (1998).
[3] B.-C. Perng and B. M. Ladanyi, "Longitudinal dielectric properties of molecular liquids: Molecular dynamics simulation studies of CH3CN, C6H6, and CO2," The Journal of Chemical Physics **110**, 6389–6405 (1999).
[4] P. Kakkar, A. O'Neil, and A. Travesset, "Water Dielectric Function at Finite Wavelength and the Convergence of Its Large Wavelength Limit (Static

Dielectric) by Fluctuation Formulas," The Journal of Physical Chemistry A **129**, 11438–11446 (2025).

[5]H. J. Berendsen, J. R. Grigera, and T. P. Straatsma, "The missing term in effective pair potentials," Journal of Physical Chemistry **91**, 6269–6271 (1987).

[6]W. L. Jorgensen, J. Chandrasekhar, J. D. Madura, R. W. Impey, and M. L. Klein, "Comparison of simple potential functions for simulating liquid water," The Journal of Chemical Physics **79**, 926–935 (1983).

[7]H. W. Horn, W. C. Swope, J. W. Pitera, J. D. Madura, T. J. Dick, G. L. Hura, and T. Head-Gordon, "Development of an improved four-site water model for biomolecular simulations: TIP4P-Ew," The Journal of Chemical Physics **120**, 9665–9678 (2004).

[8]S. Izadi, R. Anandakrishnan, and A. V. Onufriev, "Building Water Models: A Different Approach," The Journal of Physical Chemistry Letters **5**, 3863–3871 (2014).

[9]S. W. Rick, "A reoptimization of the five-site water potential (TIP5P) for use with Ewald sums," The Journal of Chemical Physics **120**, 6085–6093 (2004).

[10]J. P. Hansen and I. R. McDonald, *Theory of Simple Liquids* (Academic Press, London, 2003).

[11]J. G. Kirkwood and F. P. Buff, "The Statistical Mechanical Theory of Solutions. I," The Journal of Chemical Physics **19**, 774–777 (1951).

[12]S. Weerasinghe and P. E. Smith, "A Kirkwood–Buff derived force field for sodium chloride in water," The Journal of Chemical Physics **119**, 11342–11349 (2003).

[13]A. Chattopadhyay, V. Mandalaparthy, and N. F. A. van der Vegt, "Determination of aqueous solubility of NaCl in molecular dynamics simulation using the Kirkwood–Buff method," The Journal of Chemical Physics **162** (2025), 10.1063/5.0264104.

[14]M. Neumann and O. Steinhauser, "On the calculation of the dielectric constant using the Ewald-Kornfeld tensor," Chemical Physics Letters **95**, 417–422 (1983).

[15]J. A. Anderson, C. D. Lorenz, and A. Travesset, "General purpose molecular dynamics simulations fully implemented on graphics processing units," Journal of Computational Physics **227**, 5342–5359 (2008), iSBN: 0021-9991.

[16]J. A. Anderson, J. Glaser, and S. C. Glotzer, "HOOMD-blue: A Python package for high-performance molecular dynamics and hard particle Monte Carlo simulations," Computational Materials Science **173**, 109363 (2020).

[17]A. Travesset, "Phase diagram of power law and Lennard-Jones systems: Crystal phases," The Journal of Chemical Physics **141**, 164501 (2014).

[18]A. Upah, A. Thomas, J. Hallstrom, and A. Travesset, "High-Precision Calculation of Nanoparticle (Nanocrystal) Potentials of Mean Force and Internal Energies," Journal of Chemical Theory and Computation **20**, 1559–1567 (2024).

[19]T. D. Nguyen, C. L. Phillips, J. A. Anderson, and S. C. Glotzer, "Rigid body constraints realized in massively-parallel molecular dynamics on graphics processing units," Computer Physics Communications **182**, 2307–2313 (2011).

[20]J. Glaser, X. Zha, J. A. Anderson, S. C. Glotzer, and A. Travesset, "Pressure in rigid body molecular dynamics," Computational Materials Science **173**, 109430 (2020).

[21]J. A. Te and T. Ichiye, "Temperature and pressure dependence of the optimized soft-sticky dipole-quadrupole-octupole water model," The Journal of Chemical Physics **132**, 114511 (2010).

[22]J. Kolafa and L. Viererblová, "Static dielectric constant from simulations revisited: Fluctuations or external field?" Journal of Chemical Theory and Computation **10**, 1468–1476 (2014).

[23]B. Hess, C. Holm, and N. van der Vegt, "Osmotic coefficients of atomistic NaCl (aq) force fields," The Journal of Chemical Physics **124** (2006), 10.1063/1.2185105.

[24]C. J. Fennell, A. Bizjak, V. Vlachy, and K. A. Dill, "Ion pairing in molecular simulations of aqueous alkali halide solutions," Journal of Physical Chemistry B **113**, 6782–6791 (2009).

[25]M. Neumann, "Computer simulation and the dielectric constant at finite wavelength," Molecular Physics **57**, 97–121 (1986).

[26]T. J. Boerner, S. Deems, T. R. Furlani, S. L. Knuth, and J. Towns, "ACCESS: Advancing Innovation," PEARC 23: Practice and Experience in Advanced Research Computing , 173–176 (2023), place: New York, NY, USA ISBN: 9781450399852.